



Effect of CO₂, nutrients and light on coastal plankton. IV. Physiological responses

C. Sobrino^{1,*}, M. Segovia², P. J. Neale³, J. M. Mercado⁴, C. García-Gómez², G. Kulk⁵,
M. R. Lorenzo², T. Camarena^{6,7}, W. H. van de Poll⁵, K. Spilling^{6,7}, Z. Ruan^{8,9}

¹Department of Ecology and Animal Biology, Faculty of Sciences, University of Vigo, Campus Lagoas-Marcosende s/n, 36310 Vigo, Spain

²Department of Ecology, Faculty of Sciences, University of Málaga, Bulevar Louis Pasteur s/n, 29071 Málaga, Spain

³Smithsonian Environmental Research Center, Edgewater, Maryland 21037, USA

⁴Spanish Institute of Oceanography, 29640 Fuengirola, Spain

⁵Department of Ocean Ecosystems, Energy and Sustainability Research Institute Groningen, University of Groningen, 9747 AG Groningen, The Netherlands

⁶Finnish Environment Institute, Marine Research Center, 00251 Helsinki, Finland

⁷Tvärminnen Zoological Station, University of Helsinki, 10900 Hanko, Finland

⁸Marine Biology Institute & Guangdong Provincial Key Laboratory of Marine Biotechnology, Shantou University, Shantou, Guangdong 515063, China

⁹Dipartimento di Scienze dell'Ambiente e della Vita, Università Politecnica delle Marche, via Brecce Bianche, 60131 Ancona, Italy

ABSTRACT: We studied the physiological response of phytoplankton to the interacting effects of 3 factors affected by global climate change: CO₂, nutrient loading and irradiance. Treatments had a high and low level for each factor: CO₂ was bubbled at 1000 ppm by volume versus present atmospheric values; high nutrient treatments had a combination of inorganic and organic nutrients; and light treatments were obtained by covering the tanks with a single or double layer of screen. We measured esterase activity, oxidative stress (ROS), cell death, DNA damage, photosynthetic efficiency and ¹⁴C assimilation as particulate or dissolved organic material (POC and DOC respectively). Conditions simulating future global change scenarios showed similar chlorophyll-normalized primary productivity as present conditions. The main effect driving phytoplankton physiology was the downregulation of the photosynthetic apparatus by elevated CO₂, which decreased esterase activity, ROS, cell death and DNA damage. Nutrient concentration and light acted as additional modulators, upregulating or contributing to downregulation. The percentage of DO¹⁴C extracellular release (PER) was low (0 to 27 %), significantly lower under ultraviolet radiation (UVR) than under photosynthetically active radiation (PAR), and acted mainly to re-equilibrate the internal balance when cells grown under UVR were exposed to PAR. PER was almost 3 times lower under high CO₂, confirming a higher resource use efficiency of phytoplankton under future CO₂ concentrations.

KEY WORDS: CO₂ · Downregulation · Nutrients · Microcosms · Photosynthesis · Phytoplankton · Ultraviolet radiation

INTRODUCTION

Despite the considerable contribution of marine phytoplankton to global climate and biogeochemical cycles, many aspects of their ecology and physiology in future global change–ocean biology relationships

are poorly understood. In general terms, phytoplankton growth and productivity rely on 2 growth-limiting environmental factors: light and nutrients. In excess, these factors can also have negative effects on phytoplankton performance. High irradiances and/or the ultraviolet (UVR) component of solar radiation (290 to

*Corresponding author: sobrinoc@uvigo.es

400 nm) can be deleterious for phytoplankton (see review by Vincent & Neale 2000). Nutrient deprivation can cause reduced physiological rates, and ultimately, shut-down of physiological processes resulting in cell death (Berges & Falkowski 1998). But increased runoff as expected from global change (Oki & Kanae 2006) can also impair phytoplankton physiology and community structure in coastal areas, as the runoff transports increased amounts of allochthonous organic and inorganic nutrients and toxicants from expanding urban, industrial and agricultural activities (Gruber & Galloway 2008). Additionally, although dissolved inorganic carbon (DIC) is in most cases not a limiting resource for marine phytoplankton, a better understanding is still needed regarding the effects of continuing uptake of CO₂ into the ocean, with consequences for the partitioning of DIC between CO₂ and HCO₃⁻. CO₂ can diffuse passively through the cell membrane, whereas HCO₃⁻, which is more abundant than CO₂ and occurs in higher concentrations than necessary for photosynthesis, needs active CO₂ concentrating mechanisms (CCMs) (see reviews by Price et al. 1998, Kaplan & Reinhold 1999, Giordano et al. 2005). Most phytoplankton species have active CCMs under present CO₂ concentrations, but down-regulation of CCM activity is expected for the high CO₂ levels predicted in future climate scenarios (Berman-Frank et al. 1998, Tortell et al. 2000, Tortell & Morel 2002).

Global change also affects exposure of phytoplankton in surface waters to solar UVR penetration through changes in the mixing depth, stratospheric ozone concentration, cloud cover and changes in the coloured part of dissolved organic matter (CDOM) (Moran & Zepp 1997, Zepp et al. 2007). The latest reports indicate that global warming will continue to cool the stratosphere, making ozone destruction more prevalent even as the volume of chlorofluorocarbons in the stratosphere is slowly reduced (Shanklin 2010). From a physiological point of view, solar radiation can have a range of inhibitory effects on phytoplankton, including UVR inhibition of nutrient uptake, damage to DNA and damage to light transduction and carbon assimilation mechanisms (Vincent & Neale 2000, Helbling & Zagarese 2003, Häder et al. 2007). UVR effects on DNA generate several photoproducts which affect replication and transcription of the DNA, causing mutations and/or cell death. The 2 major classes of mutagenic DNA lesions induced by UVR in phytoplankton are cyclobutane pyrimidine photodimers (CPDs) and the 6-4 photoproducts (6-4PPs) (van de Poll et al. 2002). Excessive solar radiation can be indicated by increased mem-

brane permeability, changes in cell elemental composition and decreased growth, among others (Buma et al. 1996, Gieskes & Buma 1997, Sobrino et al. 2004). Cell photodamage can be minimised by the protective or repairing activity of cell enzymes, including superoxide dismutase, ascorbate peroxidase and catalase involved in scavenging reactive oxygen species (ROS), and lyases, polymerases or ligases involved in DNA repair (Rijstenbil 2002, García-Gómez et al. 2012, Bouchard et al. 2013). Cellular repair processes depend on ATP supply, and on nitrogen and phosphorus for protein re-synthesis; as a consequence, final response showing the balance between damage and cellular repair may depend on nutrient availability (Litchman et al. 2002). In addition to inorganic nutrients, organic compounds can act as a very efficient source of matter for de novo synthesis of cellular components arrested by photodamage. In contrast to nutrient availability, high CO₂ concentrations seem to increase the sensitivity of phytoplankton to high solar irradiance (Sobrino et al. 2008, 2009, Gao et al. 2009, 2012, Wu et al. 2012). The response has been related to a downregulation of the photosynthetic machinery by high CO₂ levels, which reduces the incorporation and synthesis of new metabolic components, thus reducing intracellular pools, and therefore reducing compounds involved in repair mechanisms (Sobrino et al. 2008, 2009). However, some contrasting responses have also been observed (Sobrino et al. 2005a, García-Gómez et al. 2014) and further information about the molecular mechanisms and the consequences of downregulation for cell metabolism is still needed (Raven 1991, Hopkinson et al. 2010, Kim et al. 2013).

Natural environments are characterized by the presence of continuous interactions of multiple factors, or drivers, making it difficult to understand, and more difficult to predict, effects at an ecosystem level (Boyd & Hutchins 2012). Under this scenario, experimental approaches trying to simulate the interactive effects of multiple environmental factors and their effects on phytoplankton physiology are essential to understand the responses of planktonic communities (Litchman et al. 2012). Among those, elevated CO₂, increases in inorganic and organic nutrients and irradiance availability have been described as some of the significant factors for phytoplankton in coastal waters (Gruber & Galloway 2008, Beardall et al. 2009). In the present study, we aimed to investigate the interactive effects of these 3 environmental factors, paying special attention to the role of UVR. We focused on the allocation of organic carbon produced by phytoplankton as particulate (POC) or dissolved

(DOC) material as an important physiological process with relevance for trophic interactions and biogeochemical cycles. The release of DOC from phytoplankton represents a carbon loss from the cells and explains, together with respiration and grazing, the uncoupling between production and biomass. DOC is a significant source of carbon for bacterial metabolism (Cogg 1983, Fole et al. 1988) and has been related to UVR stress in oligotrophic lakes and marine waters (Carrillo et al. 2002, Helbling et al. 2013).

MATERIALS AND METHODS

The results of this study are part of an experiment conducted during the Group for Aquatic Productivity (GAP) 9th international workshop. We have divided the presentation of the results of the overall experiment into a series of 4 reports. The papers from Neale et al. (2014a) and Mercado et al. (2014, both this Theme Section) show the results from the physicochemical and biological variables respectively, and the paper from Reul et al. (2014, this Theme Section) shows changes in taxonomic composition. In the present report, we focus on the physiological responses by analysing of esterase activity, oxidative stress and cell death (by using fluorescence probes), DNA damage (immunodetection), photosynthetic efficiency (maximum quantum yield for Photosystem II) and ¹⁴C assimilation by phytoplankton (POC, DOC, and percentage of extracellular release, PER). A summary of the whole set of variables measured during the entire experiment is shown in Neale et al. (2014a, their Table 2).

Experimental setup

Experimental design and sampling procedures were performed as described in detail in Neale et al. (2014a). Briefly, the experiment measured variation in the characteristics of coastal phytoplankton and bacterioplankton incubated under 8 treatments over a 7 d period. Treatments represented the full factorial combinations of 2 levels each of nutrient concentrations, CO₂ supply and solar radiation exposure. Nutrient additions were a combination of inorganic and organic nutrients simulating the effects of coastal eutrophication as previously described by Martínez-García et al. (2010) (high nutrients, HN vs. low nutrients, LN; i.e. natural concentrations). All microcosms were continuously aerated at a constant flow rate of ca. 100 ml min⁻¹ with either ambient air (low CO₂,

LC) or air that was enriched with CO₂ to a level of 1000 ppm by volume (ppmv; high CO₂, HC), as the value predicted for future scenarios of global change (IPCC 2013). Flow rate was controlled with individual flow meters (Aalborg) and CO₂ supply was provided from a gas tank. High light microcosms (HL) were covered with a single layer of nylon screen and low light microcosms (LL) had a double layer of nylon screen. The usage of the density screens produced 2 different irradiance treatments, while avoiding unrealistic excessive damage in cells grown under static conditions (i.e. not mixed in the water column).

Water samples were collected from a coastal station in the Alborán Sea (southwest Mediterranean Sea, 36.54° N, 4.60° W) on Day -1 (15 September 2012), screened through a 200 µm mesh to remove mesozooplankton (see Neale et al. 2014 for details), combined in a shaded mixing tank and then dispensed into microcosms consisting of UVR-transparent low density polyethylene (LDPE) 20 l bags ('cubitainers'). The bags were suspended in 4 large tanks (approximately 800 l) and sampled each morning of the following 7 d (Days 0 through 6; 16 through 22 September). There were 3 replicate microcosms per treatment, with 2 treatments located in each 800 l tank. Samples used for the measurements reported in the present study were collected around 09:00 h using an acid-washed glass tube connected to a clean silicone tube under manual vacuum with a syringe. In case the analysis was not performed immediately, collected samples were maintained in the dark in a walk-in chamber at a constant temperature similar to the tank temperature (<3 h).

The water sample collected on Day -1 was low in nutrients as is typical for this region of the Mediterranean. For the nutrient enriched treatments, 3 µM nitrate and 0.2 µM phosphate was added on Day 0 to bring the initial N:P ratio to 11:1. Additional phosphate was added on Day 2 as needed in order to restore a near 11:1 N:P ratio. Clear sky conditions prevailed with some mist and fog in the mornings. Average midday photosynthetically active radiation (PAR) in the microcosms was 539 and 232 µmol m⁻² s⁻¹ for HL and LL respectively, and total UV exposure (290 to 400 nm) for this midday period ranged between 7.4–22.7 W m⁻² (HL) and 3.9–11.9 W m⁻² (LL) (Neale et al. 2014a). See Table 1 for PAR and UVR values for Days 0, 2, 4 and 6, when all the variables shown in the present paper were measured. Average ± SE pCO₂ in the HC and LC microcosms was 1050 ± 70 and 453 ± 11 ppmv respectively, reflecting the experimental targets of 1000 ppmv in the enhanced CO₂ treatments versus present values

Table 1. Photosynthetically active radiation (PAR) and ultraviolet radiation (UVR) irradiance reaching the incubated samples after correction by the Ultraphan 295 and Lee-226 films, FEP bottle and screen factor, using light data from Neale et al. (2014a). PAR is shown as the mean (\pm SD) irradiance and the minimum and maximum values observed, as well as total doses during the incubation. In addition, we show un-weighted irradiance and predicted ratios of photosynthetic rates under UVR irradiances divided by maximum photosynthetic rates (P/P_{\max} , dimensionless) using the biological weighting functions for the inhibition of photosynthesis of *Synechococcus* grown under medium and high light (Neale et al. 2014b), and for the diatom *Thalassiosira pseudonana* (Sobrinho et al. 2008)

	Day 0 (16 Sep 2012)	Day 2 (18 Sep 2012)	Day 4 (20 Sep 2012)	Day 6 (22 Sep 2012)
PAR				
Irradiance ($\mu\text{mol photons m}^{-2} \text{ s}^{-1}$)	1361 \pm 237	449 \pm 127	871 \pm 463	990 \pm 120
Min.–max. ($\mu\text{mol photons m}^{-2} \text{ s}^{-1}$)	927–1668	311–765	400–1601	757–1129
Dose (fluence in kJ m^{-2})	3196	1053	2046	2766
UVR				
Unweighted irradiance (W m^{-2})	36.1 \pm 7.5	12.7 \pm 3.2	24.9 \pm 12.7	28.1 \pm 3.4
P/P_{\max} <i>Syn</i> medium light	0.57 \pm 0.04	0.72 \pm 0.03	0.63 \pm 0.08	0.60 \pm 0.03
P/P_{\max} <i>Syn</i> high light	0.64 \pm 0.05	0.80 \pm 0.03	0.71 \pm 0.09	0.68 \pm 0.03
P/P_{\max} <i>T. pseudonana</i>	0.71 \pm 0.04	0.85 \pm 0.03	0.77 \pm 0.08	0.75 \pm 0.03

(380 ppmv) in the treatments aerated with ambient air (Neale et al. 2014a). Chlorophyll *a* (chl *a*) concentration showed a steady increase in all treatments from 0.85 $\mu\text{g l}^{-1}$ on Day –1 to 4.39 ± 1.4 on Day 6, with the most rapid growth and highest chl *a* occurring in the HN treatments (Neale et al. 2014a). In terms of abundance, a positive response to increased CO_2 and nutrient concentration was observed during the first 2 d in all chlorophyll size fractions (<2, 2 to 20 and >20 μm), but mainly in the <2 μm fraction. It was followed by a bloom of nano- and microplankton diatoms on Day 4, dominated by *Leptocylindrus danicus* and *Chaetoceros* sp. Contribution of diatoms to plankton biomass decreased on Day 6 due to both silicate depletion and the increase of the small cell fraction. In terms of biomass, >20 μm autotrophic cells were the main plankton fraction during the whole experiment (Mercado et al. 2014, Reul et al. 2014).

***In vivo* chl *a* fluorescence**

Maximum photosynthetic efficiency (quantum yield) of Photosystem II (PSII) (F_v/F_m) was measured daily with a Water PAM fluorometer (Walz). Samples collected from each microcosm in the morning were maintained in the dark at room temperature for approximately 20 min before measurements of F_v/F_m values. F_v/F_m is described as $(F_m - F_o)/F_m$, where F_v is the variable fluorescence of a dark-adapted sample, F_m is the maximum fluorescence intensity with all PSII reaction centres closed, and F_o is the minimum fluorescence.

Esterase activity, oxidative stress and cell death

Samples for the assessment of esterase activity, cell death and oxidative stress were collected from each microcosm on Days 0, 2, 4 and 6 in 50 ml Falcon tubes and analyzed in triplicate by using a microplate fluorescence reader (FL-600, BIO-TEK). Fluorescence emission from the microplate reader was confirmed by flow cytometry (FACSort flow cytometer, BD Biosciences). Negative controls were run to check for artifactual fluorescence. These controls consisted of 0.2 μm filtered seawater both with and without each of the different fluorescent probes. Controls consisting of experimental samples without the fluorescent probes were also measured.

Non-specific cell esterase activity from each microcosm was analyzed by using fluorescein diacetate (FDA) (#F1303, Invitrogen) as described by Segovia & Berges (2009). Fluorescence emission after cleavage of fluorescein and diacetate molecules has been related to photosynthetic activity measured by ^{14}C and metabolic vigor under PAR and UVR exposures (Dorsey et al. 1989, Sobrinho et al. 2004). FDA was added to 1.5 ml samples at 20 μM final concentration. Samples were incubated at 20°C in darkness for 60 min. Fluorescence was detected using the microplate fluorescence reader at an excitation of 451 nm and an emission of 510 nm.

ROS were analyzed using a modification of the method used by Segovia & Berges (2009) described in Bouchard et al. (2013). Briefly, ROS detection was performed using carboxy- H_2DFFDA (Invitrogen). Cells were incubated in darkness with 5 μM c- H_2DFFDA

(final conc.) at 20°C for 90 min. Green fluorescence was detected as described above by using the microplate fluorescence reader at an excitation of 492 nm and an emission of 517 nm.

Cell death was assessed using the nucleic acid stain Sytox-Green (Invitrogen) according to Segovia & Berges (2009). Briefly, 5 µM final concentration was added to 1.5 ml sample and incubated at a temperature close to the experimental conditions (20°C) in darkness for 60 min. Fluorescence was quantified in the microplate fluorescence reader at an excitation of 490 nm and an emission of 525 nm. Positive controls consisting of 100% killed cells were run in parallel and obtained by pre-treating the samples with 2% glutaraldehyde (final conc.) at 4°C for 120 min.

DNA damage

DNA damage was assessed in samples collected on Days 0, 4 and 6 by using a modification of the protocol from Boelen et al. (1999) as described in García-Gómez et al. (2012). For this purpose, samples (1 to 2 l) were collected from each microcosm and gently filtered through 0.8 µm polycarbonate filters. Samples were snap frozen in liquid nitrogen and kept at -80°C until analysis. For analysis, DNA was extracted and quantified from the filters; 15 ng of DNA were used from each sample for immunodetection of CPDs with a monoclonal anti-CPD antibody (H3, Affitech).

Photosynthetic production of POC and DOC

Parallel incubations were carried out to measure the photosynthetic production of POC and DOC under PAR and PAR+UVR exposures. These incubations were performed on Days 0, 2, 4 and 6 starting around noon and lasting for 3 to 3.5 h. Samples (30 ml) of each microcosm were inoculated with H¹⁴CO₃⁻ (approximately 1 µCi ml⁻¹ final conc.) and incubated in UVR-transparent Teflon-FEP bottles under PAR and PAR+UVR exposures in a temperature-controlled tank contiguous to the experimental microcosms. The Teflon bottles were tied on top of UVR-transparent acrylic trays, keeping all bottles under flat and constant position. Trays were wrapped with LEE-226 (LEE Filters: 92% of transmittance, T, at 700 nm and 50% T at 400 nm) and with Ultraphan 295 (Digefra: 93% T at 700 nm and 50% T at 295 nm) cut-off filters to achieve PAR (i.e. excluding UVR) and UVR (i.e. UVR and PAR included) conditions respectively (herein PAR for only PAR irradiance and UVR for

PAR+UVR). One dark control per treatment (8 in total) was maintained under the same incubation conditions. In order to avoid excessive solar radiation so that results would be more representative of surface layer responses, trays were covered with 1 layer of neutral density screen during clear-sky days (Days 2 and 6). See Table 1 for PAR and UVR irradiances reaching the samples after correction by the Ultraphan 295 and 395 films, FEP bottle and screen factor (%T = 69%). Un-weighted and weighted UV irradiances using the biological weighting functions for the inhibition of photosynthesis from cultures of *Synechococcus* under low light and high light, and for the diatom *Thalassiosira pseudonana* are also included (Sobrino et al. 2008, Neale et al. 2014b).

For analysis of the fraction of fixed carbon incorporated into POC and DOC, 5 ml samples were filtered through 0.2 µm polycarbonate filters (25 mm diameter) under low pressure (50 mm Hg) after the light incubation period, using 3 manifolds simultaneously (10 positions per manifold). POC was retained on the filter, whereas the filtrate was directly collected in scintillation vials to assess ¹⁴C activity in the dissolved fraction (i.e. DOC). Non-assimilated ¹⁴C was released by exposing the filters to acid fumes (50% HCl) or by adding 200 µl of 10% HCl to the filtrates and shaking overnight. The radioactivity of each sample was measured using a scintillation counter LS-6599 (Beckman). The PER was calculated as the ratio of DOC divided by the sum of DOC and POC (total organic carbon fixed, TOC). In addition, measurements of TOC were performed on Days 4 and 6 (n = 29) to test differences between non-filtered samples (including both particulate and dissolved material) and filtered samples. There was no significant difference between measurements of TOC compared with the sum of the particulate and dissolved fractions (p = 0.47, n = 29).

To compare DOC release under PAR and UVR exposures with cell health, the cell digestion assay (Agustí & Sánchez 2002) was used to assess membrane permeability and cell viability. Samples (5 ml) from each replicate microcosm were combined and incubated in Teflon bottles simultaneously with the POC-DOC incubations. After PAR and UVR exposure, 1 ml from the mixed sample was incubated with 150 µl DNase I solution for 15 min at 37°C. Then, 150 µl Trypsin solution was added and the samples were incubated for 30 min at 37°C. After incubation, samples were fixed with 1% formalin (final conc.), snap frozen in liquid nitrogen, and stored at -80°C until further analysis. Cell density was analyzed within 48 h after exposure using a FACSCalibur flow cytometer (BD Biosciences). Viability measured as

the % of living cells was then calculated by dividing the cell density obtained after the cell digestion assay (living cells) by the cell density in the samples collected prior to exposure to PAR and UVR (total cells) and multiplied by 100.

Statistical analyses

Differences due to the effects of CO₂, nutrients and light were tested by 3-way ANOVA or 1- or 2-way repeated measures ANOVAS followed by post hoc Holm-Sidak or Tukey tests, respectively (considering $p \leq 0.05$ as significant). Data were checked for homogeneity of variances and normality using Levene's and Kolmogorov-Smirnov tests, respectively. When appropriate, some of the data were tested for significance of differences ($p < 0.05$) promoted by the treatments using Student's *t*-tests. Statistical analyses were carried out by using the Systat statistical package included in Sigmaplot v.11 (Systat Software).

RESULTS

In vivo chl *a* fluorescence associated to PSII (F_v/F_m)

Maximum photosynthetic efficiency measured as F_v/F_m was within the typical range of healthy cells (mean \pm SD: 0.63 ± 0.03 ; min. = 0.57, max. = 0.67) during the whole experiment (Fig. 1). F_v/F_m values showed that growth conditions of the original coastal water sample (kept in a shaded tank from Day -1 to Day 0) corresponded to those in the LC LN LL treatment on Day 1 (Fig. 1). The exposure to higher irradiance on Day 1 (a sunny day) lowered the F_v/F_m in all treatments except in the HC LL treatments, which showed higher F_v/F_m (Holm-Sidak, $p = 0.039$). Irradiance was lower on Day 2, leading to a recovery from this initial stress. Then from Day 2 to Day 4, F_v/F_m decreased in all the treatments except LC LN LL, but recovered again at the end of the experiment.

Esterase activity, oxidative stress and cell death

Values decreased linearly in most of the treatments from Day 2 to Day 6 for all 3 variables (Fig. 2). The main exception was

the LC LN LL treatment, which showed an opposite trend and had the lowest values of esterase activity and ROS on Day 2 but increased significantly on Day 4, finally resulting in the treatment with one of the highest values of esterase activity, ROS and cell death on Day 6 (Fig. 2C,F,I).

Compared to values before incubation, esterase activity on Day 2 increased in the high light treatments (Holm-Sidak, $p = 0.035$) but decreased under low light ($p = 0.025$), while ROS increased ($p < 0.0001$) and cell death decreased ($p = 0.0005$) in all the treatments (Fig. 2).

The esterase activity (Fig. 2A–C) was highly affected by irradiance, but an inverse pattern was observed between HC and LC treatments regarding nutrient effects: under HC conditions, the nutrient additions produced similar or higher activity only under HL conditions. In contrast, under LC conditions, the nutrient addition only increased esterase activity under LL. This pattern was observed for the HC treatments during the whole experiment but was only apparent under LC conditions on Day 2. Variability and differences among treatments within HC and LC conditions decreased from Day 2 to Day 6.

ROS results (Fig. 2D–F) on Day 2 did not show a pattern indicating a clear interaction with nutrients and light such as that observed for the esterase activity. However, under LC conditions, the LN HL treatment showed the highest, and the LN LL the lowest value of ROS. This pattern reversed afterwards for

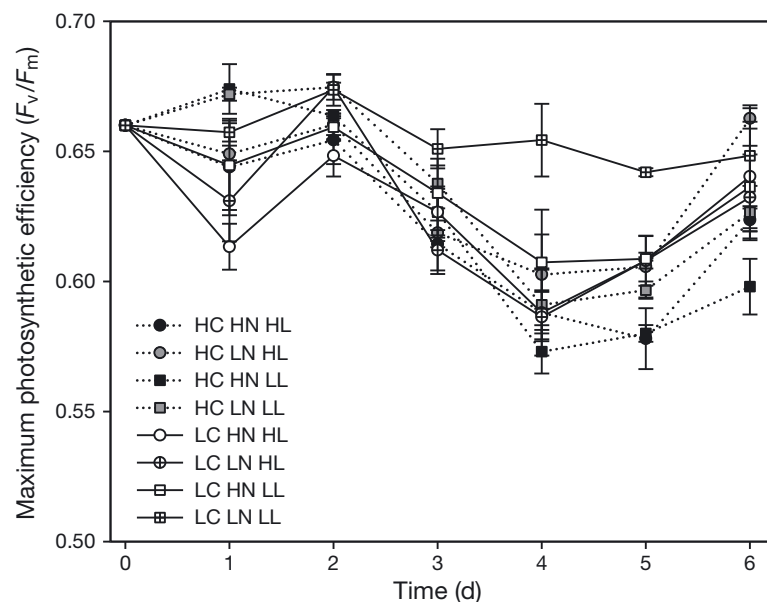


Fig. 1. Changes in the mean (\pm SE, $n = 3$) maximum quantum yield of PSII of phytoplankton exposed to the interactive effects of high (H) and low (L) levels of CO₂ (C), nutrients (N) and light (L) measured with a pulse amplitude modulated (PAM) fluorometer during the microcosm experiment



Fig. 2. Changes in mean (\pm SE, $n = 3$) chl-*a*-normalized esterase activity, reactive oxygen species (ROS; c-H₂DFFDA) and cell death (Sytox) (relative fluorescence units, R.F.U.) by Day 2 (left), Day 4 (middle) and Day 6 (right) of phytoplankton exposed to the interactive effects of high or low (H or L) levels of CO₂ (C), nutrients (N) and light (L). Dashed horizontal line shows values of the phytoplankton community before the incubation (Day -1). Continuous vertical line separates HC treatments (left) from LC treatments (right), with additional gray or white fill for distinction; open and cross-hatched boxes on top of each figure indicate HL and LL treatments respectively; dotted and solid fill indicate HN and LN treatments respectively

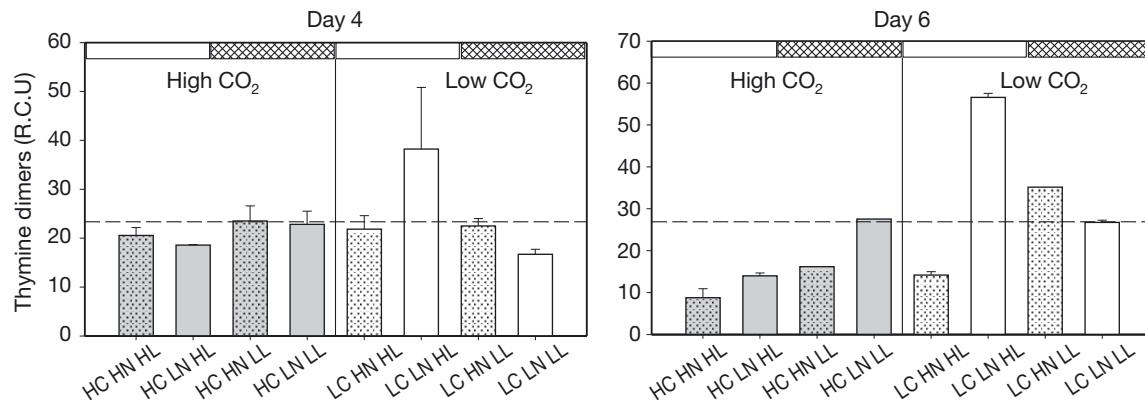


Fig. 3. Changes in mean (\pm SE, $n = 3$) DNA damage measured as cyclobutane pyrimidine dimer (CPD) accumulation (relative chemiluminescence units, R.C.U.) by Day 4 (left panel) and Day 6 (right panel) of phytoplankton exposed to the interactive effects of high or low (H or L) levels of CO₂ (C), nutrients (N) and light (L). Dashed horizontal line shows values of the phytoplankton community before the incubation (Day -1). Continuous vertical line separates HC treatments (left) from LC treatments (right), with additional gray or white fill for distinction; open and cross-hatched boxes on top of each figure indicate HL and LL treatments respectively; dotted and solid fill indicate HN and LN treatments respectively

the LN LL treatments. The treatments showed the highest ROS for both CO₂ concentrations on Day 4, and significantly higher only under HC on Day 6 (Holm-Sidak, $p = 0.0009$).

Cell death (Fig. 2G–I) was affected by nutrient loading (Holm-Sidak, $p = 0.045$) and by light mainly in the HC LN treatments ($p = 0.0002$). The pattern was maintained in the HC HL treatments on Day 4 (Holm-Sidak, $p = 0.022$) but was reversed in some and in all the treatments on Days 4 and 6 respectively; on this last day, nutrient concentration was the main factor affecting cell death (Holm-Sidak, $p = 0.02$), i.e. all the LN treatments showed higher values than the treatments with HN loading. The highest cell death on Days 4 and 6 was observed for the LC LN LL treatment.

Unlike results from Day 2, results from Day 6 were more comparable among the 3 variables, especially between the esterase activity and ROS. With the exception of cell death values for the HC HN HL treatment, all samples grown under HC conditions showed significantly lower esterase activity, cell death and presence of ROS than those grown under LC (all $p < 0.001$). Among those, low nutrient treatments showed higher values (Holm-Sidak, $p = 0.05$). Finally, light effects on this last day of incubation were only observed marginally in the LC treatments, mainly for cell death measurements.

CPD formation

Compared to non-incubated samples (i.e. samples from Day -1), CPD formation only increased in the

LC LN HL treatment on Day 4 (Fig. 3). From Days 4 to 6, damage was similar or greater in all the LC treatments except in the LC HN HL treatment, while under HC conditions, damage decreased except in the HC LN LL treatment. On Day 6, the HC HN HL treatment had the least DNA damage, whereas the LC LN HL treatment had the most (Fig. 3). HC conditions generally produced lower values of DNA damage at the end of the experiment than LC conditions (Holm-Sidak, $p \leq 0.0785$), except for the LN LL treatments that were similar between HC and LC conditions.

Photosynthetic production of POC and DOC

The chlorophyll-normalized photosynthetic production of POC under parallel incubations including PAR+UVR (i.e. similar to the microcosm incubations in UVR transparent cubitainers) on Day 2 was affected by the interaction of the 3 environmental factors (Fig. 4A). In the presence of UVR, LN treatments had the highest carbon fixation into POC (Holm-Sidak, $p = 0.042$). Among those, the HC HL treatment showed the highest carbon fixation values. These interactions were not observed on Day 4, despite receiving a higher irradiance level during the incubation (Table 1). On Day 6, only the LN LL treatments, independent of CO₂ concentrations, were significantly higher ($p = 0.037$). On Day 6, cells from the LN and LL treatments assimilated 70% more POC under UVR than those from other treatments. In addition, cells in HC treatments showed on average 12% lower POC assimilation compared to those in

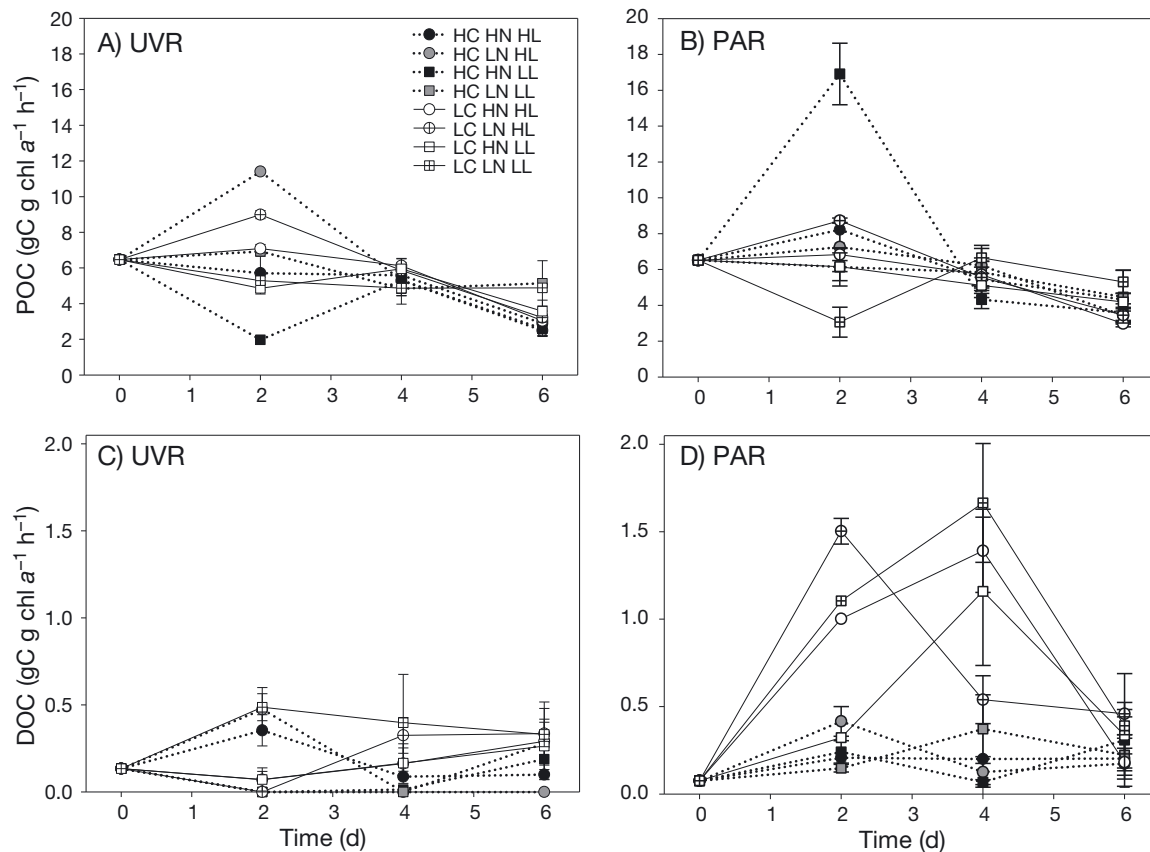


Fig. 4. Changes in mean (\pm SE, $n = 3$) photosynthetic production of particulate organic carbon (POC) and dissolved organic carbon (DOC) measured by ¹⁴C of phytoplankton exposed to the interactive effects of high or low (H or L) levels of CO₂ (C), nutrients (N) and light (L). Incubations were carried out under natural radiation conditions including (A,C) the whole solar spectrum (including UVR), or (B,D) excluding UVR (photosynthetically active radiation only, PAR)

LC treatments, although this difference was not statistically significant.

When UVR was excluded from the spectrum, HC treatments on Day 2 had higher carbon fixation compared to LC treatments, except the LN HL treatment (Fig. 4B). The HC HN LL treatment had the highest carbon fixation into POC, while the lowest was found under LC LN LL conditions. There were no significant differences among treatments from this day to the end of the experiment, although, similar to those under UVR exposures and to the results observed with the fluorescent probes, the LC LN LL had the highest value on Day 6. Particulate carbon fixation correlated with esterase activity ($R^2 = 0.62$, $n = 18$; data not shown). Correlation decreased if the analysis included the 'extreme' conditions (i.e. the HC HN HL and LC LN LL treatments), which had higher and lower esterase activity respectively, than expected by ¹⁴C assimilation per se. Conversely, the correlation increased if only values from the initial phase of the experiment (i.e. Day 2) were compared ($R^2_{\text{Day2}} = 0.75$, $n = 6$; data not shown).

The fraction of fixed C released as DOC was approximately 12 times lower than the fraction incorporated into POC, and responded in a very different way. The release of radiolabeled DOC was higher under low CO₂ than under high CO₂ conditions (t -test, $p = 0.0008$), mainly on Days 2 and 4 under PAR exposures. Furthermore, phytoplankton DOC production was much lower under UVR than under PAR (t -test, $p = 0.0014$) (Fig. 4C,D). A similar trend, with higher DOC production under low CO₂ was also observed under UVR exposures on Days 4 and 6 (Fig. 4C). Among PAR-exposed samples, LC LN treatments had the highest DOC release on Day 2, and more under HL than under LL. However, under UVR, the HL treatment (i.e. LC LN HL) had significantly lower DOC release (t -test, $p = 0.0063$) than the LL treatment (i.e. LC LN LL), which showed one of the highest values during the whole experiment. On Day 4, a day with higher irradiance than Day 2 (Table 1), the release of DOC in the treatments with LN and HL decreased abruptly under PAR, and variability of the results increased significantly. All LC treatments de-

Table 2. Mean (\pm SEM, $n = 3$) percentage of DO^{14}C extracellular release (PER) of dissolved organic carbon, and percentage viability measured by the cell digestion assay (CDA) analysis depending on light spectra (photosynthetically active radiation, PAR vs. whole solar spectrum, UVR) and CO_2 , nutrient and light (irradiance) conditions

Factor	Treatment	PER	Ratio PER	%Viability	Ratio viability
Light spectrum	PAR	8.58 ± 1.37	2.36 ± 0.91	86.1 ± 4.5	1.12 ± 0.11
	UVR	3.63 ± 0.66		76.9 ± 6.6	
CO_2	Low	9.15 ± 1.37	2.98 ± 0.66	77.5 ± 6.8	0.91 ± 0.09
	High	3.07 ± 0.50		85.5 ± 4.4	
Nutrients	Low	6.74 ± 1.33	1.23 ± 0.34	85.0 ± 6.9	1.09 ± 0.11
	High	5.48 ± 1.06		78.0 ± 4.2	
Irradiance	Low	6.41 ± 1.36	1.10 ± 0.31	83.0 ± 4.5	1.04 ± 0.10
	High	5.80 ± 1.04		80.1 ± 6.7	

creased DOC release from Day 4 to Day 6, showing values similar to those in the HC treatments (Fig. 4D).

PER ranged from 0 to 27 %, with responses similar to those observed for DOC (Table 2, Fig. 4). Averaging all data, CO_2 was the factor with the highest effect on PER, which was almost 3 times higher under LC than under HC conditions (t -test, $p = 0.0001$)

(Table 2). Nutrient loading and irradiance treatments did not show significant differences between high and low conditions (Table 2). Light spectra had also a very important effect, as cells exposed to PAR had approximately 2 times higher PER than those exposed to PAR+UVR (t -test, $p = 0.0021$) (Table 2). As a consequence, phytoplanktonic production of TOC normalized by chlorophyll, as the sum of DOC and POC, was 15% higher under PAR-exposed samples than in samples where UVR was excluded (data not shown). DOC showed 12 times higher UV-photoinhibition than POC production, which ranged from 2 to 17% photoinhibition.

However, due to the low values of the dissolved compared to the particulate fraction, POC and DOC contributed 60 and 40% respectively to TOC decrease under UVR.

Contrary to phytoplanktonic DOC release, cell viability measured in these samples using the cell digestion assay was not affected by CO_2 , nutrients or light

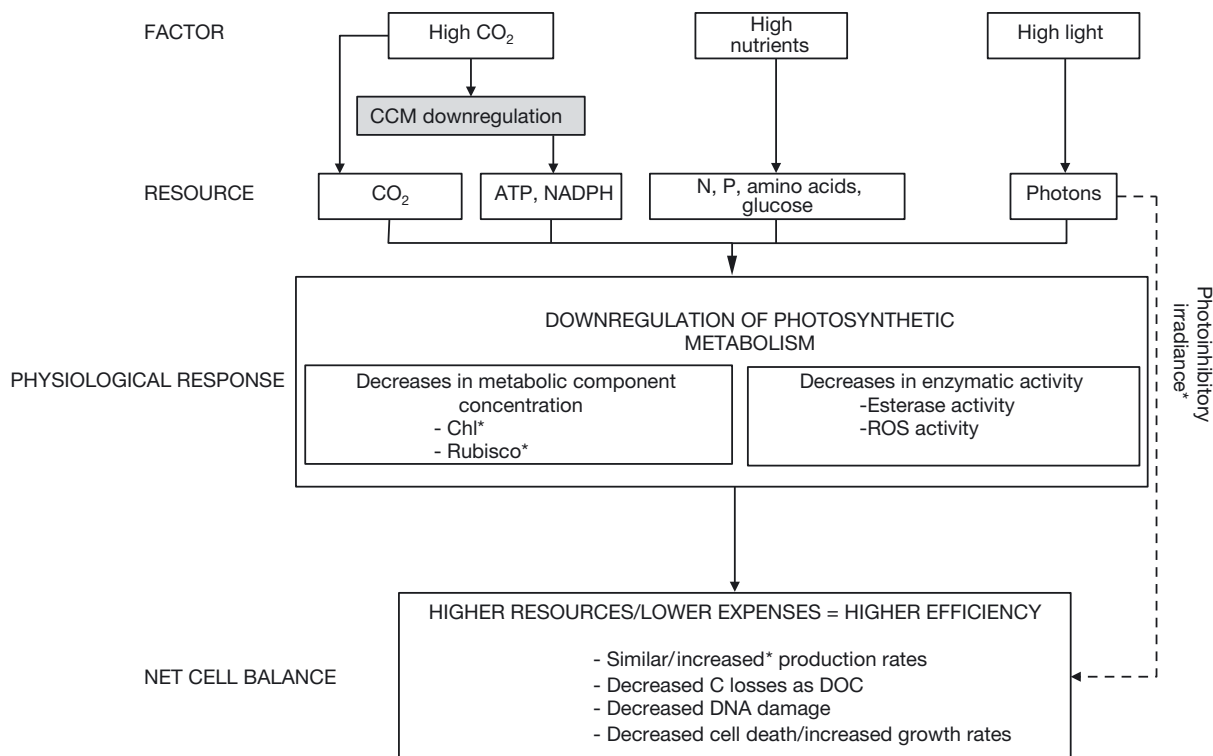


Fig. 5. Conceptual model showing the cascading effects produced by high CO_2 , high nutrients and high light availability on phytoplankton metabolism from the results obtained in this study. Grey shading highlights the importance of CCM (carbon concentrating mechanism) downregulation on other processes of the conceptual model (i.e. energy savings, downregulation of the photosynthetic metabolism and cell efficiency). Asterisks indicate results that have been obtained from other studies. Dashed line indicates negative effects

spectra and intensity (Table 2). Cell viability was very similar among all treatments on any one day. Average values for all treatments showed a mean (\pm SEM) percentage of living cells of 97 ± 7 , 63 ± 4 and 85 ± 6 for Days 2, 4 and 6, respectively, and demonstrated that the higher DOC release in some treatments was not related to increased membrane permeability or cell mortality.

DISCUSSION

Experimental setup and phytoplankton response

Our experimental approach analysed the molecular and physiological responses of phytoplankton exposed simultaneously to 3 important environmental factors related to global climate change: elevated CO₂, high loading of organic and inorganic nutrients, and varying PAR and UVR irradiance. These responses overlay concomitant taxonomic and size changes in the microcosm assemblages, although diatoms were the main plankton fraction contributing to total biomass during the whole experiment (Mercado et al. 2014, Reul et al. 2014). Throughout all these changes, and probably due to ongoing physiological acclimation, chl *a* steadily increased over time in all the treatments, with nutrient addition further stimulating growth (Neale et al. 2014a). Nutrient concentration was also the main driver for changes in bulk phytoplanktonic production rates (Mercado et al. 2014). However, this response was uncoupled from that observed for biomass, which reached a peak on Day 4 in most of the treatments probably due to interactions with CO₂ and light (Mercado et al. 2014). We report here the physiological processes that interact from the molecular to the organism level, helping to understand the final response of the phytoplankton community at each stage of the experiment.

F_v/F_m values indicated that the original coastal phytoplankton assemblage was acclimated to environmental conditions corresponding to present atmospheric levels of CO₂ (i.e. 380 ppmv) and low nutrient concentrations. Apparently, an overnight stay in the shaded mixing tank had also allowed this assemblage to recover from any effects of an average surface layer irradiance that was 85 % of incident irradiance (discussed in more detail in Neale et al. 2014a). The exposure of the original coastal water to the experimental conditions produced small inhibitory effects at the beginning of the incubation due to high light. This was reflected in the maximum photosyn-

thetic efficiency, the cellular esterase activity and the production of DOC, but did not affect the production of metabolic components such as chl *a* (Neale et al. 2014a). High F_v/F_m values during the rest of the experiment also indicate that the experimental conditions used for the study were not detrimental for the cells, keeping them under realistic conditions regarding light spectra and irradiance, nutrient and CO₂ concentrations. However, changes were very modest, and values of F_v/F_m were unexpectedly high, especially for those cells that were likely experiencing nutrient limitation at the end of the experiment. A possible explanation for the modest changes in F_v/F_m may be related to our early morning sampling protocol, which would minimize light effects and acclimation to nutrient limitation as explained by Mercado et al. (2014).

Metabolic activity and cell damage

Previous studies have demonstrated a covariation of esterase activity (FDA fluorescence) and maximum ¹⁴C fixation with changes in cell volume (Dorsey et al. 1989) and between cell size-normalized esterase activity and chl *a* fluorescence (Sobrino et al. 2005b). Recently, it has been reported that the TWCA1, a group of carbonic anhydrases present in many marine phytoplankton, possesses both CO₂ hydration and esterase activity (Lee et al. 2013), indicating that esterase activity in phytoplankton is highly related to the carbon acquisition metabolism in the cell.

Our results agree with the cited reports, indicating that phytoplankton esterase activity mainly reflects carbon fixation-related processes, but they also demonstrate that esterase activity depends on the basal metabolism and the acclimation state of the cells. Therefore, metabolic (esterase) activity remains in steady state when cells are well acclimated and not affected by stressful or disturbing conditions. The opposite occurs when one or more drivers exert effects on the cells. Following with this contention, esterase activity decreased proportionally more than carbon fixation with acclimation to the experimental conditions that occurred from the start to the end of the experiment. More importantly, it decreased more in those treatments where the resource availability exceeded the demand. This is demonstrated in our results by the lower esterase activity values under high CO₂ compared to low CO₂ conditions, and lower values under high nutrient compared to low nutrient conditions. It is also important to note that the reduced esterase response for downregulated healthy

cells differs from that observed in toxicological studies where a decrease in esterase activity is related to the impairment of cell metabolism due to acute damage (Hampel et al. 2001, Hadjoudja et al. 2009, Eigemann et al. 2013). Low light conditions in our study were already within the range of saturating irradiances, while high light conditions were potentially photoinhibitory at midday since the LDPE cubitainers were UVR-transparent. The most significant response was, however, exerted by elevated CO₂, probably due to the close relationship between esterase activity and photosynthetic metabolism (Dorsey et al. 1989, Sobrino et al. 2005b, Lee et al. 2013). Downregulation of the photosynthetic apparatus under high CO₂ conditions has been proposed as an important metabolic process, but the physiological mechanisms and its consequences for the biogeochemical cycles are only starting to be understood (Raven 1991, Sobrino et al. 2008, 2009, Beardall et al. 2009, Hopkinson et al. 2010, Kim et al. 2013). It will be considered with more detail later in the discussion.

The presence of ROS in our results closely matches that observed for the esterase activity. Significantly higher concentrations of ROS are usually linked to disturbing, usually photoinhibitory, conditions (Rijstebil 2002, Bouchard et al. 2013, García-Gómez et al. 2014). But ROS production also correlates with growth metabolism during a diel cycle, similarly to other metabolic and enzymatic activities under non-stressful conditions (Kim et al. 2004, Sobrino et al. 2004). In our results, ROS production was higher due to both high light and the synergy of high light and low nutrient conditions at the beginning of the experiment. Low nutrient conditions may reduce cellular repair in UVR-exposed phytoplankton (Litchman et al. 2002), probably increasing ROS production as observed for natural phytoplankton communities under high light and nutrient limiting conditions (Kim et al. 2005, Cartaxana et al. 2013). However, that response was counteracted by the presence of high CO₂, which decreased ROS concentration compared to cells acclimated to present levels of CO₂. The CO₂ effect on ROS—just like the esterase activity—was observed during the whole experiment, but increased as cells became more acclimated. In fact, the effect of light on ROS almost disappeared after the first days of the experiment while CO₂ effects remained and even became more significant at the end of the experiment.

The presence of ROS was not correlated with the production of CPDs, which were less variable than the esterase activity, ROS production and cell death. Dominance of photoinhibition over DNA damage has

already been described under several mixing conditions of solar exposures (Helbling et al. 2008) and seems to be supported by the results of the present study. Under acclimated conditions, DNA damage was higher under low light conditions, probably due to photoenhancement of the repair in high light-acclimated phytoplankton (Buma et al. 2003). The exception to this was the LC LN LL treatment, which also had an outlying response in the other measured variables. The response of this treatment seems to be related to a reduced growth rate caused by the limiting conditions. This was reflected in lower biomass and nitrate uptake rates in LC LN LL than in the other treatments (Mercado et al. 2014), despite no changes in terms of carbon fixation into POC or lower chlorophyll compared to the other LN treatments (Neale et al. 2014a). Comparison of cellular responses associated with photoenhanced repair and nucleotide excision ('dark') repair has indicated that light-mediated correction of UV damage is an important factor in the number of photoproducts induced and cell survival (Karentz et al. 1991). Additionally, lower DNA damage under high CO₂ conditions can be related to the lower production of ROS observed in acclimated cells, since a decrease in ROS can indirectly decrease damage to DNA. Some studies have also shown a direct relationship between the number of photoproducts and cell survival (Karentz et al. 1991, Boelen et al. 2000, Buma et al. 2001, Meador et al. 2009), but this relationship was not observed in our results when cell death was measured with the Sytox fluorescence probe. In our study, the nutrient addition affected the extent of cell death more than the DNA damage in acclimated phytoplankton. Cell death was more closely related to the metabolic activity (i.e. esterase activity and ROS) of the cells. However, similar to CPD production, cell death was higher under low irradiances, but only when CO₂ levels were also low. No significant differences were observed under high CO₂ regarding high light effects on cell death despite high CO₂ and high light levels also causing significant decreases in cumulative biomass (Mercado et al. 2014). One of the drawbacks of growing cells under a basal metabolism favoured by downregulated conditions is that cells are not able to cope with damage as fast as under active metabolic status. If other stressors such as high irradiance (Wu et al. 2010, Gao et al. 2012) and UVR (Sobrino et al. 2008, 2009, Gao et al. 2009, Wu et al. 2012) affect cells under these conditions, it is likely that they will cause higher damage than under 'non relaxing' conditions. Even though lack of clear photoinhibition indicates that cells were highly acclimated

to high solar irradiance in this experiment, it is likely that UVR damage on different targets than those reported in this manuscript was too acute to be counteracted under downregulated conditions. The results from the present study confirm previous statements from Sobrino et al. (2008, 2009), who proposed that a downregulated metabolism would have relatively lower amounts of enzymes involved in the repair process of UVR-caused damage or a lower activation state of the general defense mechanism (e.g. lower cellular concentrations of superoxide dismutase and ascorbate peroxidase) (Lesser 1996). They demonstrate that a reduced amount or activity of esterases and ROS under high CO₂ conditions can increase susceptibility to UVR in coastal phytoplankton communities, as previously observed for cultures of a marine diatom and natural lake assemblages (Sobrino et al. 2008, 2009).

Photosynthetic production of POC and DOC

The fact that high CO₂ concentrations did not produce higher primary production normalized by chlorophyll was probably due to interactions among the environmental drivers. The values we obtained are within the range of or lower than those observed in other marine coastal waters from temperate areas (Villafañe et al. 2004, 2013). This may be explained by the high cellular capability of acclimation to high solar irradiances typical from the studied area and summer season (Morán & Estrada 2001, Guan & Gao 2008). Still, some differences were observed at the beginning of the experiment, demonstrating the importance of UVR as an ecological factor in aquatic ecosystems: the treatment under HC HN LL had nearly a 9-fold increase in POC fixation when UVR was excluded compared to the value under UVR. Additionally, when the whole light spectrum was present (similar to that in the LDPE cubitainers), there were some stimulatory effects of photosynthesis in the treatments with low nutrients, which may be due to photochemistry increasing the availability of otherwise recalcitrant metabolites (Moran & Zepp 1997). Our results (see also Neale et al. 2014a) indicate that for those LN treatments, high light but also high CO₂ increased carbon fixation due to photodegradation, and probably to an acceleration of the activity of bacterial extracellular enzymes under high CO₂ conditions (Piontek et al. 2010).

In contrast to our results, elevated CO₂ has frequently been observed to enhance photosynthetic rates in natural marine phytoplankton assemblages

(Hein & Sand-Jensen 1997, Tortell & Morel 2002, Egge et al. 2009, Engel et al. 2013), although carbon assimilation was measured under spectra that did not include UVR in these studies. However, similar to our results, Tortell et al. (2000) did not find any stimulation of phytoplankton production in response to elevated CO₂. The most plausible explanation for having higher productivity under high CO₂ levels is that external, high CO₂ concentrations increase passive diffusion and reduce the amount of energy and metabolites necessary to drive the active transport of C to Rubisco, leaving this energy for other growth-related mechanisms (Raven 1991). Although the total amount of energy that is saved under these conditions has not been calculated, it has been estimated that the energy expended in the CCMs can be approximately 20% of the total energy used for carbon fixation (Raven 1991). The CO₂ concentrations used in this study (i.e. similar to future scenarios of global change) have resulted in downregulation of CCMs in marine phytoplankton species, such as diatoms and haptophytes (Tortell et al. 2000, Rost et al. 2003, Mercado et al. 2014). Energy savings from downregulation of the CCMs is likely the main reason for the downregulation of the photosynthetic and further cellular metabolism (Fig. 5).

Furthermore, lower POC production in the HC treatments compared to the LC treatments under the full solar spectrum (including UVR) indicates that downregulation also increases photoinhibition, in agreement with the responses observed from the esterase activity, ROS production and cell death. In contrast, low CO₂ conditions induce active CCMs, which maintain a constant flow of C to Rubisco but with high energetic demand. Only when metabolism faces an environmental challenge, for example the limitation of additional resources such as nutrients or photons, do cells display a stimulatory effect under high CO₂ conditions. It is important to recall that these responses are observed in cells acclimated to high CO₂ levels and differ from those observed at the beginning of the experiment, when cells are still adapting to the new conditions (Sobrino et al. 2008). Acclimation rate to elevated CO₂ conditions likely depends on metabolic rates, and therefore on environmental conditions. Factors such as low temperature can slow down the rate of acclimation to high CO₂, producing significant responses of downregulated cells over longer time scales than observed in this study (Egge et al. 2009, Hopkinson et al. 2010). For temperatures similar to those recorded in this study (20 to 24°C), 3 or 4 d are enough to reach downregulated conditions (Sobrino et al. 2008, 2009).

Unlike POC, the production of DOC from phytoplankton photosynthesis is usually considered one of the main carbon and energy losses (together with respiration and grazing), and has been frequently used to explain the uncoupling between assimilated carbon (i.e. photosynthesis) and biomass in studies aimed to understand CO₂ effects on phytoplankton (Riebesell et al. 2007, Hopkinson et al. 2010). Our results are in agreement with Hopkinson et al. (2010) in that high CO₂ levels reduce cellular carbon loss. However, in our case as in other studies, the response is linked mainly to low nutrient concentrations, rather than to nutrient replete conditions (Berman-Frank & Dubinsky 1999, Pausz & Herndl 1999, Conan et al. 2007, López-Sandoval et al. 2011). These results are contrary to those reported by Engel (2002) and Borchard & Engel (2012), showing higher DOC production and transparent exopolymer polysaccharides (TEPs) under high CO₂ conditions. From a physiological perspective, the fraction of phytoplanktonic carbon released as DOC in our study seems to be an active mechanism to re-equilibrate the internal balance, which is uncoupled from POC fixation at this experimental scale (Berman-Frank & Dubinsky 1999). High rates of active CO₂ uptake are out of balance with carbon assimilation rates if the assimilation during the dark reactions of photosynthesis is constrained by low nutrient availability. The role of light on DOC production depends on total irradiance and spectral distribution being stimulatory under saturating and non-inhibitory exposures (Morán & Estrada 2001, Panzenböck 2007), probably because carbon uptake by CCMs is modulated by light (Bartual & Galvez 2003, Chen & Gao 2004), sometimes at higher rates than required for carbon fixation (Tchernov et al. 1998). In contrast, photons in excess or with high energy per wavelength (i.e. UVR) result in opposite responses.

Passive diffusion would be another mechanism of DOC release if membrane permeability increased due to low pH, nutrient starvation or photoinhibitory light conditions. However, our results using a membrane permeability-dependent test indicate a clear lack of relationship between both processes independent of the environmental factors. Interestingly, UVR inhibition of DOC release was 2 times higher under low CO₂ conditions, when cells potentially have active CCMs, than under high CO₂ conditions. The lack of significant cellular damage in response to UVR throughout the whole experiment, plus the fact that DOC release occurred during the initial and intermediate phases of the experiment, suggest that elevated release of phytoplanktonic DOC was re-

lated to a lessening in UVR-mediated pressure—as opposed to a direct damaging effect by UVR—when cells coming from UVR conditions in the LDPE cubitainers were exposed to less stressful PAR conditions (Beardall et al. 2002). Such relief is likely exerted on the same photosynthetic component that creates the imbalance under low nutrient conditions, but further molecular analysis should be carried out to reach a definitive conclusion. Our results differ from previous studies that show higher extracellular DOC release caused by UVR in phytoplankton from lakes and oligotrophic marine waters (Carrillo et al. 2002, Helbling et al. 2013). Despite the very different environments, both are characterized by having phytoplankton living under high UVR doses, low nutrient concentrations and normally constant, relatively high CO₂ levels. In fact, average PER values in our study are low compared to values from oligotrophic areas where DOC release has been directly related to cell lysis (Agustí & Duarte 2013), but are similar to those observed in healthy cells from coastal, nutrient replete areas (Conan et al. 2007, Wetz & Wheeler 2007).

CONCLUSIONS

A conceptual model that summarizes the effects of the 3 environmental factors tested in this study on phytoplankton physiology and net metabolic balance is shown in Fig. 5. We found that the main physiological effect of the interaction of elevated CO₂, nutrient concentration and light on coastal phytoplankton was the downregulation of the photosynthetic metabolism mediated by elevated CO₂ concentrations, which affects the whole cellular physiology. This was demonstrated in our study by decreased cell esterase activity, ROS and cell death, as well as decreased DNA damage under high CO₂ conditions. In addition to CO₂, nutrient concentration and light functioned as important modulators upregulating as well as contributing to the downregulation of the cell metabolism. Downregulation of cell metabolism under high CO₂ made cells more susceptible to photoinhibition than cells with higher activity rates, finally resulting in similar or lower primary production and biomass. In contrast, high CO₂ under non-photoinhibitory exposures increased biomass (Mercado et al. 2014). One of the most important findings of the present study was the role of DOC release as an active mechanism to re-equilibrate the internal balance of phytoplankton cells under the combined influence of the environmental factors. Such re-

equilibration seemed to be more necessary in cells under low CO₂ compared to high CO₂ concentrations due to the lower resource use efficiency in cells that are potentially using active CCMs (Mercado et al. 2014). Higher DOC release under low CO₂ compared to high CO₂ conditions explains the uncoupling between production and biomass in our experiment to some extent (see also higher respiration rates in Mercado et al. 2014). Our results also showed that UVR can potentially decrease TOC production by 15% in phytoplankton from coastal waters acclimated to high solar irradiance, where UVR also acts as an important environmental modulator with effects on photobiology and photochemistry.

Acknowledgements. The experiments were performed in the framework of the workshop GAP9 that was partially financed by the University of Málaga (Program 'Plan Propio'). We are extensively grateful for the logistic and technical support from the Centro Oceanográfico de Málaga (Instituto Español de Oceanografía).

LITERATURE CITED

- Agustí S, Duarte CM (2013) Phytoplankton lysis predicts dissolved organic carbon release in marine plankton communities. *Biogeosciences* 10:1259–1264
- Agustí S, Sánchez MC (2002) Cell viability in natural phytoplankton communities quantified by a membrane permeability probe. *Limnol Oceanogr* 47:818–828
- Bartual A, Galvez JA (2003) Short- and long-term effects of irradiance and CO₂ availability on carbon fixation by two marine diatoms. *Can J Bot* 81:191–200
- Beardall J, Heraud P, Roberts S, Shelly K, Stojkovic S (2002) Effects of UV-B radiation on inorganic carbon acquisition by the marine microalga *Dunaliella tertiolecta* (Chlorophyceae). *Phycologia* 41:268–272
- Beardall J, Sobrino C, Stojkovic C (2009) Interactions between the impacts of ultraviolet radiation, elevated CO₂, and nutrient limitation on marine primary producers. *Photochem Photobiol Sci* 8:1257–1265
- Berges JA, Falkowski PG (1998) Physiological stress and cell death in marine phytoplankton: induction of proteases in response to nitrogen or light limitation. *Limnol Oceanogr* 43:129–135
- Berman-Frank I, Dubinsky Z (1999) Balanced growth in aquatic plants: myth or reality? *Bioscience* 49:29–37
- Berman-Frank I, Erez J, Kaplan A (1998) Growth of dinoflagellates as influenced by the availability of CO₂ and inorganic carbon uptake in a lake ecosystem. *Can J Bot* 76:1043–1051
- Boelen PI, Obernoster I, Vink A, Buma AGJ (1999) Attenuation of biologically effective UV radiation in tropical Atlantic waters measured with a biochemical DNA dosimeter. *Photochem Photobiol* 69:34–40
- Boelen P, de Boer MK, Kraay GW, Veldhuis MJW, Buma AGJ (2000) UVBR-induced DNA damage in natural marine picoplankton assemblages in the tropical Atlantic Ocean. *Mar Ecol Prog Ser* 193:1–9
- Borchard C, Engel A (2012) Organic matter exudation by *Emiliania huxleyi* under simulated future ocean conditions. *Biogeosciences* 9:3405–3423
- Bouchard JN, García-Gómez C, Lorenzo MR, Segovia M (2013) Differential effect of ultraviolet exposure (UVR) in the stress response of the Dinophyceae *Gymnodinium* sp. and the Chlorophyta *Dunaliella tertiolecta*: mortality versus survival. *Mar Biol* 160:2547–2560
- Boyd PW, Hutchins DA (2012) Understanding the responses of ocean biota to a complex matrix of cumulative anthropogenic change. *Mar Ecol Prog Ser* 470:125–135
- Buma AGJ, Zemmellnk HJ, Sjollem K, Gieskes WWC (1996) UVB radiation modifies protein and photosynthetic pigment content, volume and ultrastructure of marine diatoms. *Mar Ecol Prog Ser* 142:47–54
- Buma AGJ, de Boer MK, Boelen P (2001) Depth distributions of DNA damage in Antarctic marine phyto- and bacterioplankton exposed to summertime ultraviolet radiation. *J Phycol* 37:200–208
- Buma A, Boelen P, Jeffrey WH (2003) UVR-induced DNA damage in aquatic organisms. In: Helbling EW, Zagarese HE (eds) UV effects in aquatic organisms and ecosystems. Royal Society of Chemistry, Cambridge, p 291–327
- Carrillo P, Medina-Sánchez JM, Villar-Argaiz M (2002) The interaction of phytoplankton and bacteria in a high mountain lake: importance of the spectral composition of solar radiation. *Limnol Oceanogr* 47:1294–1306
- Cartaxana P, Domingues N, Cruz S, Jesus B, Laviale M, Serôdio J, Marques da Silva J (2013) Photoinhibition in benthic diatom assemblages under light stress. *Aquat Microb Ecol* 70:87–92
- Chen X, Gao K (2004) Characterization of diurnal photosynthetic rhythms in the marine diatom *Skeletonema costatum* grown in synchronous culture under ambient and elevated CO₂. *Funct Plant Biol* 31:399–404
- Cole JJ, Findlay S, Pace ML (1988) Bacterial production in fresh and saltwater ecosystems: a cross-system overview. *Mar Ecol Prog Ser* 43:1–10
- Conan P, Sondergaard M, Kragh T, Thingstad F and others (2007) Partitioning of organic production in marine plankton communities: the effects of inorganic nutrient ratios and community composition on new dissolved organic matter. *Limnol Oceanogr* 52:753–765
- Dorsey J, Yentsch CM, Mayo S, McKenna C (1989) Rapid analytical method for the assessment of cell metabolic activity in marine microalgae. *Cytometry* 10:622–628
- Egge JK, Thingstad TF, Larsen A, Engel A, Wohlers J, Bellerby RGJ, Riebesell U (2009) Primary production during nutrient-induced blooms at elevated CO₂ concentrations. *Biogeosciences* 6:877–885
- Eigemann F, Sabine HNK, Schmitt-Jansen M (2013) Flow cytometry as a diagnostic tool for the effects of polyphenolic allelochemicals on phytoplankton. *Aquat Bot* 104: 5–14
- Engel A (2002) Direct relationship between CO₂ uptake and transparent exopolymer particles production in natural phytoplankton. *J Plankton Res* 24:49–53
- Engel A, Borchard C, Piontek J, Schulz KG, Riebesell U, Bellerby R (2013) CO₂ increases ¹⁴C primary production in an Arctic plankton community. *Biogeosciences* 10: 1291–1308
- Fogg GE (1983) The ecological significance of extracellular products of phytoplankton photosynthesis. *Bot Mar* 26: 3–14
- Gao K, Ruan ZX, Villafañe VE, Gattuso JP, Helbling EW (2009) Ocean acidification exacerbates the effect of UV

- radiation on the calcifying phytoplankton *Emiliana huxleyi*. *Limnol Oceanogr* 54:1855–1862
- Gao K, Xu J, Gao G, Li Y and others (2012) Rising CO₂ and increased light exposure synergistically reduce marine primary productivity. *Nat Clim Change* 2:519–523
- García-Gómez C, Parages ML, Jiménez C, Palma A, Mata MT, Segovia M (2012) Cell survival after UV radiation stress in the unicellular chlorophyte *Dunaliella tertiolecta* is mediated by DNA repair and MAPK phosphorylation. *J Exp Bot* 63:5259–5274
- García-Gómez C, Gordillo FJL, Palma A, Lorenzo MR, Segovia M (2014) Elevated CO₂ alleviates high PAR and UV stress in the unicellular chlorophyte *Dunaliella tertiolecta*. *Photochem Photobiol Sci* 13:1347–1358
- Gieskes WWC, Buma AGJ (1997) UV damage to plant life in a photobiologically dynamic environment: the case of marine phytoplankton. *Plant Ecol* 128:17–25
- Giordano M, Beardall J, Raven JA (2005) CO₂ concentrating mechanisms in algae: mechanisms, environmental modulation, and evolution. *Annu Rev Plant Biol* 56:99–131
- Gruber N, Galloway JN (2008) An Earth-system perspective of the global nitrogen cycle. *Nature* 451:293–296
- Guan W, Gao K (2008) Light histories influence the impacts of solar ultraviolet radiation on photosynthesis and growth in a marine diatom, *Skeletonema costatum*. *J Photochem Photobiol B Biol* 91:151–156
- Häder DP, Kumar HD, Smith RC, Worrest RC (2007) Effects of solar UV radiation on aquatic ecosystems and interactions with climate change. *Photochem Photobiol Sci* 6:267–285
- Hadjoudja S, Vignoles C, Deluchat V, Lenain JF, Le Jeune AH, Baudu M (2009) Short term copper toxicity on *Microcystis aeruginosa* and *Chlorella vulgaris* using flow cytometry. *Aquat Toxicol* 94:255–264
- Hampel M, Moreno-Garrido I, Sobrino C, Lubián LM, Blasco J (2001) Acute toxicity of LAS homologues in marine microalgae: esterase activity and inhibition of growth as endpoints of toxicity. *Ecotoxicol Environ Saf* 48:287–292
- Hein M, Sand-Jensen K (1997) CO₂ increases oceanic primary production. *Nature* 388:526–527
- Helbling EW, Zagarese H (2003) UV effects in aquatic organisms and ecosystems. Royal Society of Chemistry, Cambridge
- Helbling EW, Buma AGJ, van de Poll WH, Fernández Zenoff MV, Villafañe VE (2008) UVR-induced photosynthetic inhibition dominates over DNA damage in marine dinoflagellates exposed to fluctuating solar radiation regimes. *J Exp Mar Biol Ecol* 365:96–102
- Helbling EW, Carrillo P, Medina-Sánchez JM, Durán C, Herrera G, Villar-Argaiz M, Villafañe VE (2013) Interactive effects of vertical mixing, nutrients and ultraviolet radiation: in situ photosynthetic responses of phytoplankton from high mountain lakes in Southern Europe. *Biogeosciences* 10:1037–1050
- Hopkinson BM, Xu Y, Shi D, McGinn PJ, Morel FMM (2010) The effect of CO₂ on the photosynthetic physiology of phytoplankton in the Gulf of Alaska. *Limnol Oceanogr* 55:2011–2024
- IPCC (2013) Climate change 2013: the physical science basis. In: Stocker TF, Qin D, Plattner GK, Tignor M and others (eds) Contribution of Working Group I to the Fifth Assessment Report of the Intergovernmental Panel on Climate Change. Cambridge University Press, Cambridge
- Kaplan A, Reinhold L (1999) CO₂ concentrating mechanisms in photosynthetic microorganisms. *Annu Rev Plant Physiol Plant Mol Biol* 50:539–570
- Karentz D, Cleaver JE, Mitchell DL (1991) Cell survival characteristics and molecular responses of Antarctic phytoplankton to ultraviolet-B radiation. *J Phycol* 27:326–341
- Kim D, Watanabe M, Nakayasu Y, Kohata K (2004) Production of superoxide anion and hydrogen peroxide associated with cell growth of *Chattonella antiqua*. *Aquat Microb Ecol* 35:57–64
- Kim D, Watanabe M, Nakayasu Y, Kohata K (2005) Changes in O₂⁻ and H₂O₂ production by *Chattonella antiqua* during diel vertical migration under nutrient stratification. *Aquat Microb Ecol* 39:183–191
- Kim JH, Kim KY, Kang EJ, Lee K and others (2013) Enhancement of photosynthetic carbon assimilation efficiency by phytoplankton in the future coastal ocean. *Biogeosciences* 10:7525–7535
- Lee RBY, Smith JAC, Rickaby REM (2013) Cloning, expression and characterization of the δ-carbonic anhydrase of *Thalassiosira weissflogii* (Bacillariophyceae). *J Phycol* 49:170–177
- Lesser MP (1996) Acclimation of phytoplankton to UV-B radiation: oxidative stress and photoinhibition of photosynthesis are not prevented by UV-absorbing compounds in the dinoflagellate *Prorocentrum micans*. *Mar Ecol Prog Ser* 132:287–297
- Litchman E, Neale PJ, Banaszak AT (2002) Increased sensitivity to ultraviolet radiation in nitrogen-limited dinoflagellates: photoprotection and repair. *Limnol Oceanogr* 47:86–94
- Litchman E, Kyle FE, Klausmeier CA, Thomas MK (2012) Phytoplankton niches, traits and eco-evolutionary responses to global environmental change. *Mar Ecol Prog Ser* 470:235–248
- López-Sandoval DC, Fernández A, Marañón E (2011) Dissolved and particulate primary production along a longitudinal gradient in the Mediterranean Sea. *Biogeosciences* 8:815–825
- Martínez-García S, Fernández E, Álvarez-Salgado XA, González J and others (2010) Differential responses of phytoplankton and heterotrophic bacteria to organic and inorganic nutrient additions in coastal waters off the NW Iberian Peninsula. *Mar Ecol Prog Ser* 416:17–33
- Meador JA, Baldwin AJ, Catala P, Jeffrey WH and others (2009) Sunlight-induced DNA damage in marine microorganisms collected along a latitudinal gradient from 70°N to 68°S. *Photochem Photobiol* 85:412–420
- Mercado JM, Sobrino C, Neale P, Segovia M and others (2014) Effect of CO₂, nutrients and light on coastal plankton. II. Metabolic rates. *Aquat Biol* 22:43–57
- Moran MA, Zepp RG (1997) Role of photoreactions in the formation of biologically labile compounds from dissolved organic matter. *Limnol Oceanogr* 42:1307–1316
- Morán XAG, Estrada M (2001) Short-term variability of photosynthetic parameters and particulate and dissolved primary production in the Alboran Sea (SW Mediterranean). *Mar Ecol Prog Ser* 212:53–67
- Neale PJ, Sobrino C, Segovia M, Mercado JM and others (2014a) Effect of CO₂, nutrients and light on coastal plankton. I. Abiotic conditions and biological responses. *Aquat Biol* 22:25–41
- Neale PJ, Pritchard AP, Ihnacik R (2014b) UV effects on the primary productivity of picophytoplankton: biological weighting functions and exposure response curves of *Synechococcus*. *Biogeosciences* 11:2883–2895

- Oki T, Kanae S (2006) Global hydrological cycles and world water resources. *Science* 313:1068–1072
- Panzenböck M (2007) Effect of solar radiation on photosynthetic extracellular carbon release and its microbial utilization in alpine and Arctic lakes. *Aquat Microb Ecol* 48:155–168
- Pausz C, Herndl GJ (1999) Role of ultraviolet radiation in phytoplankton extracellular release and its subsequent utilization by marine bacterioplankton. *Aquat Microb Ecol* 18:85–93
- Piontek J, Lunau M, Händel N, Borchard C, Wurst M, Engel A (2010) Acidification increases microbial polysaccharide degradation in the ocean. *Biogeosciences* 7:1615–1624
- Price GD, Sültemeyer D, Klughammer B, Ludwig M, Badger MR (1998) The functioning of the CO₂ concentrating mechanism in several cyanobacterial strains: a review of general physiological characteristics, genes, proteins and recent advances. *Can J Bot* 76:973–1002
- Raven JA (1991) Physiology of inorganic C acquisition and implications for resource use efficiency by marine phytoplankton: relation to increased CO₂ and temperature. *Plant Cell Environ* 14:779–794
- Reul A, Muñoz M, Bautista B, Neale PJ and others (2014) Effect of CO₂, nutrients and light on coastal plankton. III. Trophic cascade, size structure and composition. *Aquat Biol* 22:59–76
- Riebesell U, Schulz KG, Bellerby RC, Botros M and others (2007) Enhanced biological carbon consumption in a high CO₂ ocean. *Nature* 450:545–548
- Rijstenbil JW (2002) Assessment of oxidative stress in the planktonic diatom *Thalassiosira pseudonana* in response to UVA and UVB radiation. *J Plankton Res* 24:1277–1288
- Rost B, Riebesell U, Burkhardt S, Sültemeyer D (2003) Carbon acquisition of bloom-forming marine phytoplankton. *Limnol Oceanogr* 48:55–67
- Segovia M, Berges JA (2009) Inhibition of caspase-like activities prevents the appearance of reactive oxygen species and dark-induced apoptosis in the unicellular chlorophyte *Dunaliella tertiolecta*. *J Phycol* 45:1116–1126
- Shanklin J (2010) Reflections on the ozone hole. *Nature* 465:34–35
- Sobrinó C, Montero O, Lubian LM (2004) UV-B radiation increases cell permeability and damages nitrogen incorporation mechanisms in *Nannochloropsis gaditana*. *Aquat Sci* 66:421–429
- Sobrinó C, Neale PJ, Lubián LM (2005a) Interaction of UV radiation and inorganic carbon supply in the inhibition of photosynthesis: spectral and temporal responses of two marine picoplankters. *Photochem Photobiol* 81:384–393
- Sobrinó C, Montero O, Lubián LM (2005b) Effect of ultraviolet radiation on diel patterns of growth and cell viability in *Nannochloris atomus* cultures measured by flow cytometry. *Mar Ecol Prog Ser* 293:29–35
- Sobrinó C, Ward ML, Neale PJ (2008) Acclimation to elevated carbon dioxide and ultraviolet radiation in the diatom *Thalassiosira pseudonana*: effects on growth, photosynthesis, and spectral sensitivity of photoinhibition. *Limnol Oceanogr* 53:494–505
- Sobrinó C, Neale PJ, Phillips-Kress JD, Moeller RE, Porter JA (2009) Elevated CO₂ increases sensitivity to ultraviolet radiation in lacustrine phytoplankton assemblages. *Limnol Oceanogr* 54:2448–2459
- Tchernov D, Hassidim M, Vardi A, Luz B, Sukenik A, Reinhold L, Kaplan A (1998) Photosynthesizing marine microorganisms can constitute a source of CO₂ rather than a sink. *Can J Bot* 76:949–953
- Tortell PD, Morel FMM (2002) Sources of inorganic carbon for phytoplankton in the eastern Subtropical and Equatorial Pacific Ocean. *Limnol Oceanogr* 47:1012–1022
- Tortell PD, Rau GD, Morel FMM (2000) Inorganic carbon acquisition in coastal Pacific phytoplankton communities. *Limnol Oceanogr* 45:1485–1500
- van de Poll WH, Hanelt D, Hoyer K, Buma AGJ, Breeman AM (2002) Ultraviolet-B-induced cyclobutane-pyrimidine dimer formation and repair in arctic marine macrophytes. *Photochem Photobiol* 76:493–500
- Villafañe VE, Marcoval MA, Helbling EW (2004) Photosynthesis versus irradiance characteristics in phytoplankton assemblages off Patagonia (Argentina): temporal variability and solar UVR effects. *Mar Ecol Prog Ser* 284:23–34
- Villafañe VE, Banaszak AT, Guendulain-García SD, Strauch SM, Halac SR, Helbling EW (2013) Influence of seasonal variables associated with climate change on photochemical diurnal cycles of marine phytoplankton from Patagonia (Argentina). *Limnol Oceanogr* 58:203–214
- Vincent WF, Neale PJ (2000) Mechanisms of UV damage to aquatic organisms. In: de Mora SJ, Demers S, Vernet M (eds) *The effects of UV radiation on marine ecosystems*. Cambridge University Press, Cambridge, p 149–176
- Wetz MS, Wheeler PA (2007) Release of dissolved organic matter by coastal diatoms. *Limnol Oceanogr* 52:798–807
- Wu X, Gao G, Giordano M, Gao K (2012) Growth and photosynthesis of a diatom grown under elevated CO₂ in the presence of solar UV radiation. *Fundam Appl Limnol* 180:279–290
- Wu Y, Gao K, Riebesell U (2010) CO₂-induced seawater acidification affects physiological performance of the marine diatom *Phaeodactylum tricorutum*. *Biogeosciences* 7:2915–2923
- Zepp RG, Erickson DJ, Paul ND, Sulzberger B (2007) Interactive effects of solar UV radiation and climate change on biogeochemical cycling. *Photochem Photobiol Sci* 6:286–300

Submitted: December 19, 2013; Accepted: July 18, 2014

Proofs received from author(s): October 28, 2014